Materials Transactions, Vol. 43, No. 4 (2002) pp. 674 to 680

Formation of Anomalous Defect Structure on GaSb Surface by Low Temperature Sn Ion-Implantation *1

Noriko Nitta[1, *2], Masafumi Taniwaki[1], Tomoo Suzuki[1], Yoshihiko Hayashi[2], Yuhki Satoh[2] and Toshimasa Yoshiie[2]

[1]*Department of Environmental Systems Engineering, Faculty of Engineering, Kochi University of Technology, Tosayamada, Kochi 782-8502, Japan*
[2]*Research Reactor Institute, Kyoto University, Kumatori, Osaka 596-0821, Japan*

Defect formation in (100) GaSb by 60 keV Sn^+ ion-implantation at 150–153 K is investigated using cross-sectional TEM, SEM and EDX. An anomalous structure consisting of many cells, which looks like a honey comb, was formed on the surface implanted with 8.9×10^{18} ions/m^2. The diameter and the depth of a cell were about 50 nm and 220–250 nm respectively. The thickness of the walls partitioning the cells was about 10 nm. The upper part of the partitioning wall is amorphous and rich in Ga, while the lower part shows crystalline structure. A heavily strained region of 50 nm thickness, corresponding to the maximum depth of the projected Sn ions, was observed under the cells. This defect structure is compared with similar defects which have been observed in ion-implanted GaSb. The defect formation mechanism is discussed, and an explanation based on movement of the implantation induced point defects is proposed. It is assumed that hills and hollows are formed in the early stage of implantation. The point defects created on the hills do not contribute to the development of the defect structure, because they annihilate almost completely by the recombination of vacancy and interstitial and by the movement to the near surface sink. However, under the hollows, vacancies which escaped recombination remain, and the interstitial atoms, which are highly mobile at low temperatures, migrate far from there to aggregate under the hills. The hollows become deeper by the movement of the remaining vacancies to the surface, and the hills develop into the walls by the migration of the interstitial atoms from the surrounding hollows.

(Received November 26, 2001; Accepted February 15, 2002)

Keywords: *gallium antimonide, tin ion-implantation, III–V compound semiconductor, point defects, vacancy, interstitial, honey-comb, low temperature implantation, cross-sectional transmission electron microscopy, Fourier transformation, amorphous, microtwin, high resolution transmission electron microscopy, energy dispersive X-ray spectroscopy, scanning electron microscopy, anomalous behavior, swelling, elevation, cavity, void, surface defect, strain, local composition, defect structure, defect formation mechanism*

1. Introduction

Ion-implantation, which had been established for controlling the conduction type and the conductivity in Si semiconductor device processes, was applied to compound semiconductors in the later 1970s. The major interest concerned the characterization of induced defects, their formation process and their recovery by heat treatment. Nearly a decade after the frontier work by Mazey and Nelson in 1969,[1)] from the end of the 1970s to the 1980s, irradiation damage in GaAs was intensively studied using Rutherford backscattering and channeling techniques (RBS) and transmission electron microscopy (TEM) mainly by several groups in USA. This is because GaAs, having a high electron mobility, was anticipated as a major semiconductor material for high speed devices in the next generation. In the 1980s, the study was extended to other compound semiconductors such as InP due to its radiation resistance, GaP as a light emitting diode, and GaSb promising long wavelength lasers.

In the middle of the 1980s, the defect formation and recrystallization process in compound semiconductors by ion implantation were explained as follows:[2)] Amorphization occurs when damage energy accumulated in the material reaches a critical value; then by the subsequent annealing (at about 673 K) the amorphized region recrystallizes in a solid phase epitaxial manner leaving microtwins.

At the end of the 1980s, however, it was realized that the above amorphization mechanism was too simplified. Taniwaki *et al.* proposed that another important factor for amorphization is the amount of strain stored at the amorphous/crystalline interface.[3–6)] They found that amorphization occurs even at the region where the accumulated damage energy was 1/10–1/100 of the threshold displacement energy in GaAs-100 keV Sn^+[3–5)] and InP-40 keV Fe^+.[5)] In GaAs-40 keV Fe^+,[4–6)] microtwins which usually appear in recrystallization process formed in as-implanted surface, and the microtwin region transformed into amorphous structure by annealing. These results indicate that the implantation-induced stress significantly contributes to the amorphization.

Anomalous behaviors (*e.g.* surface elevation and swelling) were observed in GaSb and InSb irradiated with energetic ions. Kleitman and Yearian[7)] first observed an elevation of the surface in GaSb and InSb implanted with deuteron by the interferometery in 1957. In 1986, Homma[8)] observed filament-like microtextures in Cs^+ bombarded GaSb which developed into craters by prolonged irradiation. In 1988, Pearton *et al.*[9)] investigated production and removal of lattice damage in InAs, GaP and GaSb for implants of Si and Mg, and observed that zinc-blend type crystallites with a grain size of $\sim$17 nm remained on the implanted GaSb surface after annealing. In 1991, Callec *et al.*[10)] measured the elevations of the GaSb surface implanted under various conditions of ion species, acceleration voltage and ion doses

*1This Paper was Presented at the Autumn Meeting of the Japan Institute of Metals, held in Kanazawa, on November 22, 1999 and originally published in J. Japan Inst. Metals **64** (2000) 1141–1147.

*2Undergraduate Student, Kochi University of Technology, Present address: Graduate Student, Kochi University of Technology.

and observed their cross-sectional views by scanning electron microscopy (SEM). They considered that the elevations occurred after amorphization since the critical dose for elevation was equal to that of amorphization. In 1993, by TEM, Callec and Poudoulec[11] observed GaSb which was implanted with 1.8 MeV Ne^+ so as to create defects only in the bulk, and reported that swelling started with formation of voids and microtwins.

In this study, the defect formation and structural change in GaSb by Sn^+ ion-implantation at low temperatures were investigated mainly by utilizing cross-sectional TEM. We started this work as an extension of the research on GaAs and InP,[3–6,12] rather than focusing on the anomalous behavior in implanted GaSb. Accordingly, as factors controlling amorphization, we considered simultaneous annealing during implantation, combination of constituent elements (*e.g.* atomic mass difference between the two elements), and ion species *etc.*, in addition to the effect of the stress. In addition, we expected to find new phenomena by implantation (*e.g.* phase transformation). In the experiment, the ion implantation was performed at low temperatures in order to reduce the effect of simultaneous annealing. GaSb consisting of two elements with significantly different atomic masses, and heavy Sn ions were chosen in order to enhance the irradiation effect.

2. Experimental Procedure

From Te doped n-type GaSb wafers with the (100) orientation produced by Sumitomo Electric Industries Ltd, three samples implanted with 60 keV Sn^+ were prepared. Sample 1 for TEM observation was implanted to a dose of 8.9×10^{18} ions/m^2 at 153 K. Two other samples were for SEM observation, and the dose and substrate temperature (T_s) were 4.0×10^{18} ions/m^2 and 151 K for Sample 2, and 1.2×10^{19} ions/m^2 and 150 K for Sample 3. The as-implanted surfaces were observed with a field emission type scanning electron microscope (FE-SEM), JEOL JSM-6400F.

A cross-sectional TEM sample was prepared as follows. Two pieces of implanted wafers were bonded face-to-face with epoxy resin and Si wafers of 0.5 mm thickness were bonded on both sides. The wafers were then punched out to a 2 mm-diameter cylindrical shape by a ultrasonic disk cutter (Gatan Model 601) and inserted in a brass cylinder with a 3 mm outside diameter. A disc specimen sliced from the cylinder was mechanically ground to a thickness of 0.4 mm, followed by dimpling to a thickness of 0.2 mm by a VCR Dimpler Model D500. Finally they were thinned by ion milling with argon (Gatan Precision Ion Polishing System Model 691).

Bright and dark field images, high-resolution images and selected area diffraction patterns of the cross-section of the implanted region were observed with a field emission type transmission electron microscope (FE-TEM), JEOL JEM-2010F, and they were recorded on TEM films. The local compositions in the implanted surface were measured by an energy dispersive X-ray spectroscope (EDX), OXFORD Link ISIS, using an electron beam diameter of ϕ20 nm. Diffraction patterns for small areas (13 nm $\times$ 13 nm) were obtained by Fourier transformation (Fuji Film L process) of the lattice images with a magnification of $\times 1,000,000$ stored on imaging plates.

3. Results

3.1 TEM observation

Figure 1 shows a (110) cross-sectional view (bright field) and the selected area diffraction pattern of the GaSb implanted with 8.9×10^{18} ions/m^2 at 153 K. An anomalous defect structure is observed on the ion-implanted surface. Under the glue, there is a region with a contrast much brighter than the matrix, which seems to be thinner than the matrix. The region ranges from the surface to a depth of about 220–250 nm, which is ten times larger than the projected Sn ion range (30 nm) calculated by TRIM.[13] In this region, fibrous structures with a slightly dark contrast seem to grow along the depth direction from the matrix. A heavily strained region with 50 nm is observed at the interface between the bright contrast region and the matrix. Aggregates of point defects with about 5 nm diameters are observed to a depth of 20–30 nm under the strained region. It should be noted that we observed a similar defect structure on InSb surface implanted by Sn^+ at a low temperature.

It was first suspected that the crystal structure or the composition might differ between the bright and dark contrasts. However the structure was not different, because only the amorphous halos were observed in the selected area diffraction pattern except the spots coming from the zinc-blend type GaSb matrix, and the contrast did not change by tilting the sample. The composition profile along the depth direction was then measured by EDX.

3.2 Composition of local areas obtained by EDX

Figure 2 shows EDX spectra measured for local areas. The analyzed points range from the epoxy resin down to the deeper matrix region in alphabetical order, as indicated in the bright field image photograph. In the matrix (H), the strong peaks of Ga and Sb (the constituent elements) appear. The peak of the incident Sn atoms is hardly observed due to the overlapping with the Sb peak, and no other elements (*e.g.* carbon) were detected. In the strained region (F), intensities of Ga and Sb peaks decreased and a significant intensity of carbon was detected. This tendency was more remarkable in the bright region (B–E). In the epoxy resin (A), no indication of Ga, Sb and Sn was detected, and only the peak of carbon, the principal element of the epoxy resin, was observed. The peak of oxygen, another element of the resin, was not distinct due to the strong carbon peak nearby.

The existence of carbon in the bright contrast region indicates that the epoxy resin entered into the defect structure during the preparation of the TEM sample. From this, we conceived that the defect structure consisted of many cylindrical cavities with an open end. The bright contrast corresponds to thin regions in the anomalous structure, namely the cylindrical cavities and the dark contrast shows thick regions, namely the walls partitioning the cavities.

3.3 FE-SEM images of surface

The implanted surface was observed by FE-SEM in order to confirm that the anomalous structure consists of many cylindrical cavities. Figure 3 shows the SEM images of

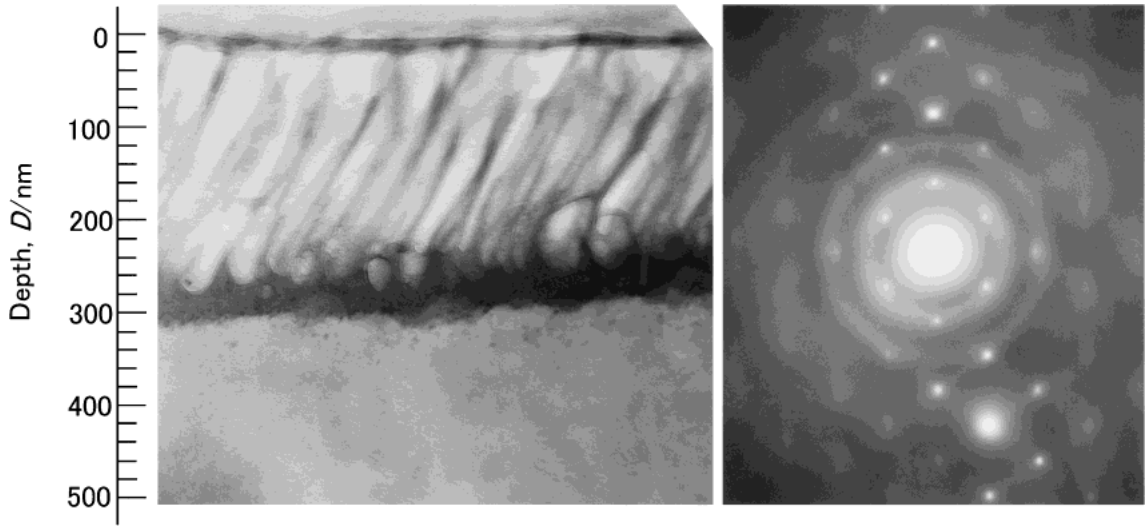

Fig. 1 The cross-sectional TEM view (bright field) and the selected area electron diffraction pattern (SAED) of GaSb surface implanted with 60 keV Sn^+ to a dose of 8.9×10^{18} ions/m^2 at 153 K. Two layers, a bright contrast region from the surface to the depth of 220–250 nm, and a heavy-strain contrast region with a 50 nm thickness under the layer are observed. Amorphous halos in SAED originate from the bright contrast region.

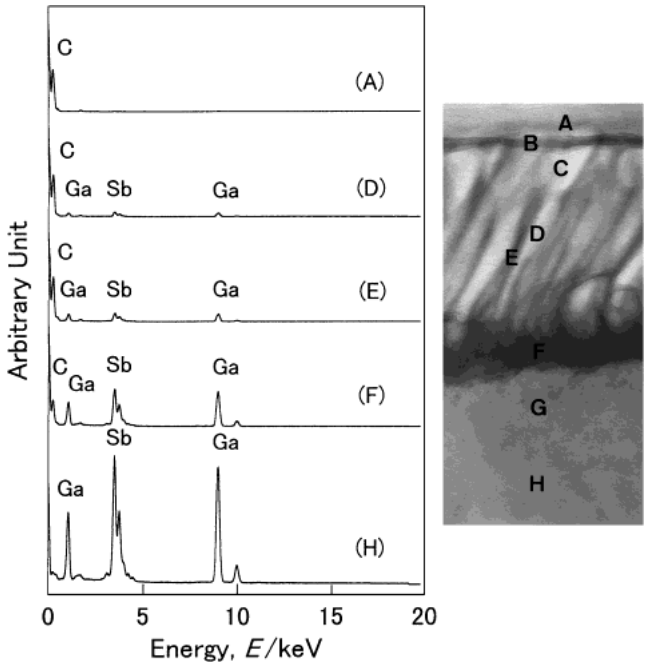

Fig. 2 EDX spectra from the local areas (ϕ20 nm) in the surface defect structure observed in Fig. 1. Analyzed spots (A-H) are shown in the TEM photograph on the right. Ga and Sb peaks are dominant in the matrix (H). Near the surface their intensities decrease and the peak intensity of C becomes strong, which shows that epoxy resin is buried in the surface.

GaSb implanted with Sn ion doses of 4.0×10^{18} ions/m^2 and 1.2×10^{19} ions/m^2. As expected, a honeycomb-like structure consisting of many cavities with thin walls is observed on the surface implanted with the larger dose. The cavity density was 3×10^{14} m^{-2}. A similar structure was formed on the surface of Sample 2 with the smaller dose, though these cavities seem to be shallower relative to those in Sample 3. The cavity density was 5×10^{14} m^{-2}, which is somewhat larger than that of Sample 3.

3.4 Detailed analysis of the defect structure

The local crystal structure in the anomalous defect was analyzed by Fourier transformation of the high resolution (HR) image, since the diameters of the selected area apertures installed in the TEM were too large to obtain the local diffraction pattern. Four HR images of the defect structure were taken on imaging plates, from which diffraction patterns of 25 local areas were obtained. Figure 4 shows several HR images and their corresponding diffraction patterns. The crystalline spots are not revealed in the upper part of the walls; however, the weak spots coinciding with those of the matrix GaSb crystal appear around the 220 nm depth from the surface, and they become clear at the lower part of the walls.

In Fig. 5, the Ga, Sb and Sn concentrations are shown as functions of the depth from the surface, where carbon was not taken into account in order to eliminate the effect the epoxy resin. The vertical axis was not calibrated, and hence the absolute value of composition was not obtained. Gallium concentration at the surface region is nearly 1.5 times larger than that of Sb. Although we could not reliably derive the distribution of Sn because of its weakness and overlap with the Sb peak, about 1 at% of Sn atoms were detected at the strained region and the top of the surface.

4. Discussion

4.1 Defect structure of surface

Figure 6 illustrates the defect structure formed on the GaSb surface implanted with 60 keV Sn^+ at a dose of 8.9×10^{18} ions/m^2. The upper picture shows the top view and the lower is the cross-sectional view. The anomalous structure consists of many cells partitioned by thin walls. The density of the cells was 3×10^{14} m^{-2}. Their diameter and depth were about 50 nm and 250 nm respectively, and the thickness of the partitioning walls was about 10 nm. The upper part of the partition is amorphous, while the lower part shows crystalline structure. The thickness of the heavily strained region under the cells is about 50 nm, which is nearly equal to the maxi-

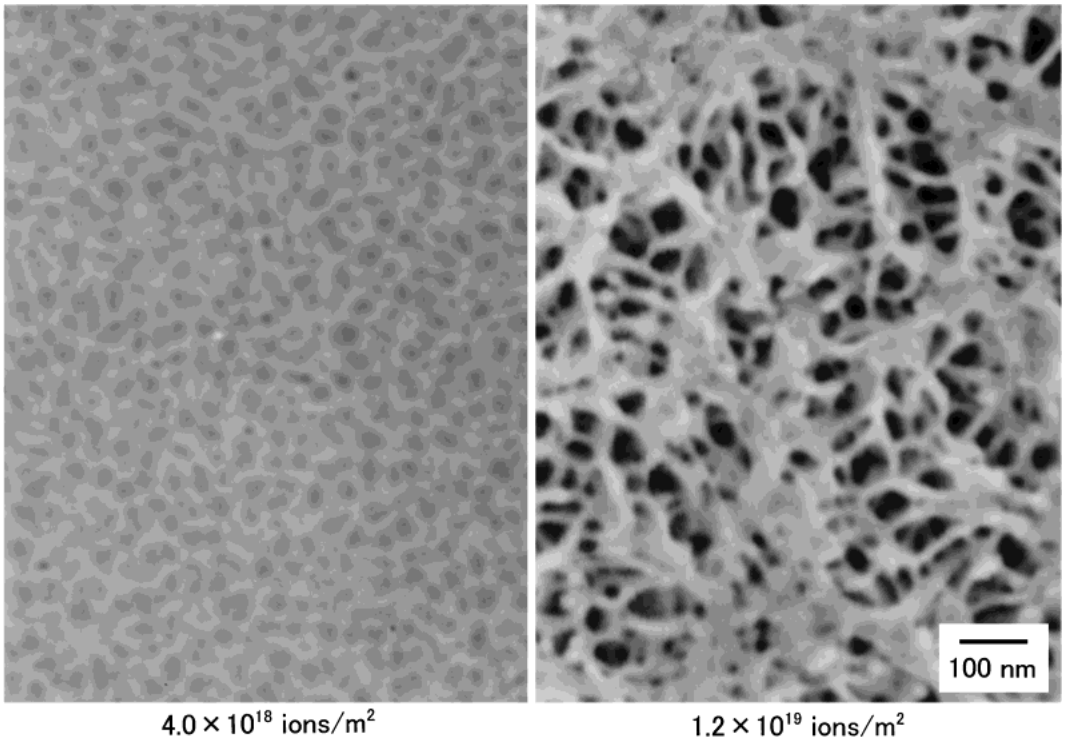

Fig. 3 FE-SEM images of GaSb surface implanted with 60 keV Sn^+. A defect structure consisting of cavities are formed; the density of cavity is 5×10^{14} m^{-2} in the sample implanted to the dose of 4.0×10^{18} ions/m^2 and 3×10^{14} m^{-2} is that of 1.2×10^{19} ions/m^2.

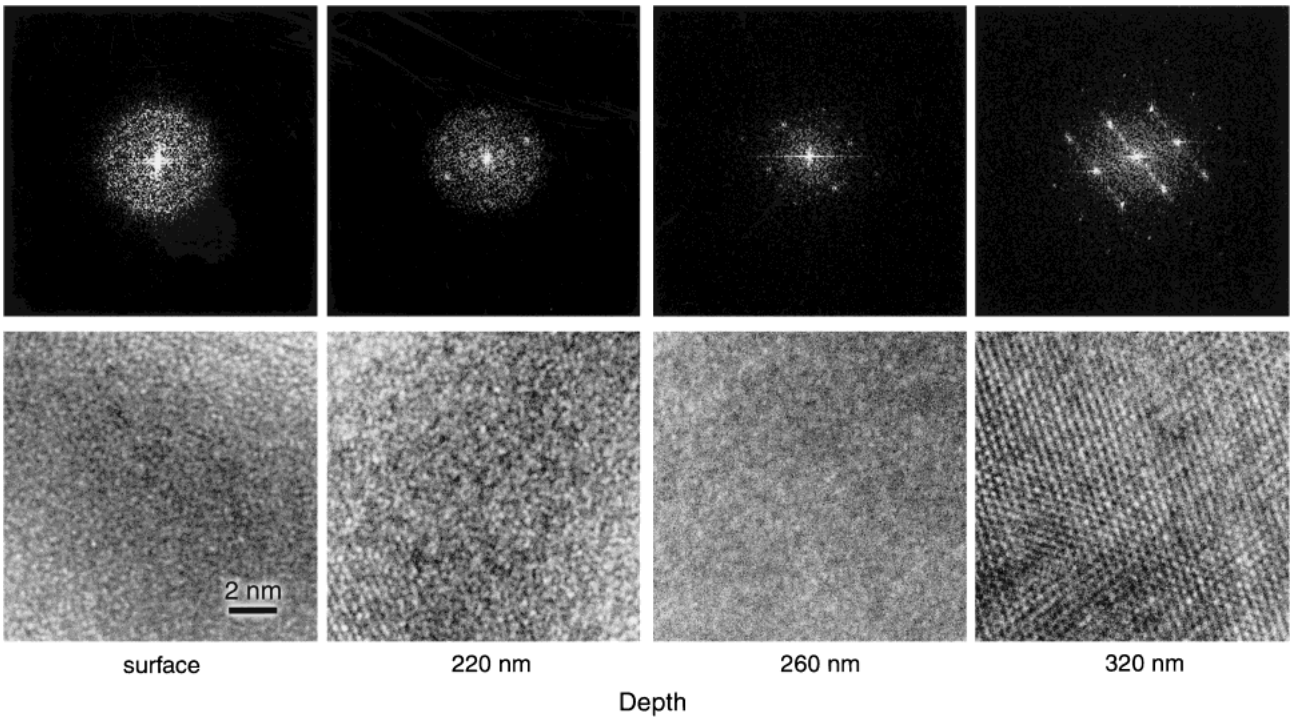

Fig. 4 Electron diffraction patterns obtained by Fourier transformation of HRTEM images are shown as a function of depth from the surface. The region near the surface is completely amorphized but the diffraction pattern of the region deeper than 220 nm reveals crystalline spots coinciding with those of the matrix.

mum depth of the projected range of the implanted Sn atoms. The composition ratio of Ga and Sb changes along the depth; Ga concentration is higher than Sb concentration in the upper part of the wall.

The anomalous defect formation behavior in Sn^+ implanted GaSb (and InSb), which has not been observed in the other compound semiconductors, seems to be related to the surface elevation in GaSb and InSb first observed by Kleitman and Yearian[7] and to the similar phenomena observed by other researchers.[8–11] However their obserred defect structures are significantly different with our found anomalous structure consisting of many cells with a high aspect ratio and with an

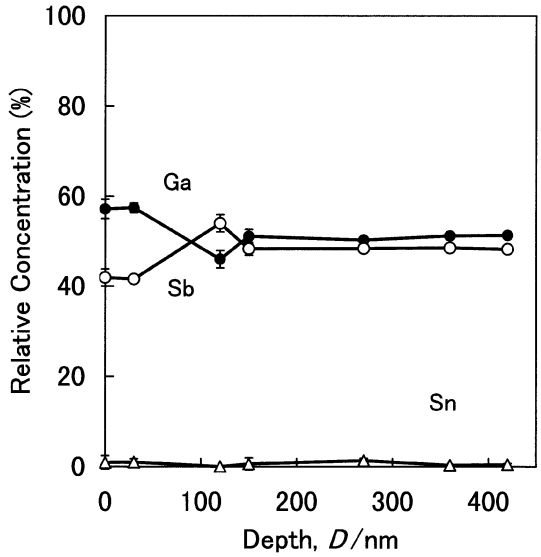

Fig. 5 Concentrations of Ga, Sb and Sn obtained form the EDX spectra are shown against the depth from the surface. Analyzed spots (B, C, D, E, F, G,H) are shown in Fig. 2. The vertical axis is not calibrated. At the surface Ga concentration increases, and is about 1.5 times as high as Sb.

open end. The sponge-like porous layer in the elevated GaSb surface observed by Callec *et al.*[10] was a pile of voids and the top surface was covered with a skin. Filament-like microtextures on Cs^+ bombarded GaSb were observed by Homma.[8] Although their SEM image shows the surface morphology somewhat similar to that in Fig. 3, the cavities were not created.

The similar defect structures were observed with SEM and cross-sectional TEM in ion implanted Ge (although it is not a compound semiconductor). Wilson[14] observed holes with 40 nm-diameter on the self-ion implanted Ge surface. They enlarged with increasing ion dose, which was eventually saturated up to about 120 nm in diameter. The TEM image of the holes resembles that of the cavities observed in the present work (Fig. 3). In the TEM study by Appleton *et al.*,[15] the Ge surface was amorphized by 120 keV In^+ implantation, and craters were created by prolonged implantation. The cross-sectional view of the layer with the craters developed by the dose of 5×10^{19} ions/m^2 is very similar to that of the anomalous defect in Fig. 1.

4.2 Formation mechanism of surface defect structure

Three possibilities are considered as a formation mechanism for the surface defect; (a) formation of the cavities by ion sputtering, (b) vapor phase growth of the walls, and (c) solid phase growth of the walls.

The mechanism (a) is almost impossible because, as shown in the SEM and TEM observation, the cavities have a depth much larger than their diameter and the partitioning walls have a very thin thickness. It is unlikely that such a uniform structure consisting of cavities with a large aspect ratio is formed directly by sputtering with the heavy implantation whose dose is nearly equal to the surface atomic density. In the mechanism (b), the vapor of Ga or Sb must be supplied to the sample; however, it is impossible for the constituent elements to evaporate at the substrate temperature of 150 K. Thus the possibility of vapor phase growth can also be excluded. Accordingly, only the solid phase growth of walls (c) remains.

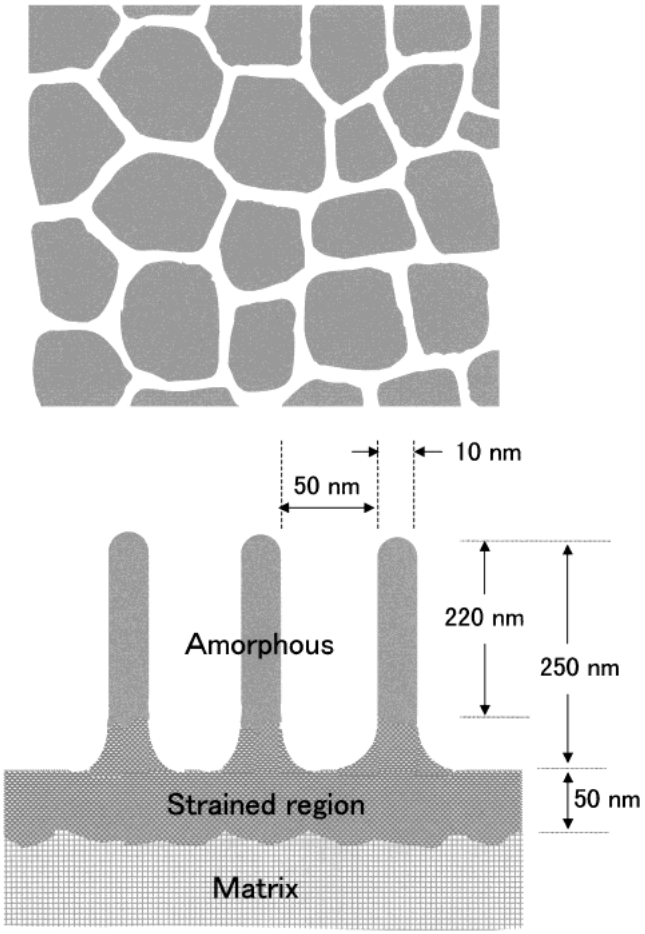

Fig. 6 Defect structure formed on the GaSb surface implanted with 60 keV Sn^+ to a dose of 8.9×10^{18} ions/m^2. The upper picture shows the top view and the lower one is the cross-sectional view.

We propose a formation mechanism based on movement of the implantation-induced point defects as shown in Fig. 7. It is assumed that hills and hollows are formed at the early stage of implantation. Tin ion implantation creates vacancies and interstitials under the surface (to a depth of about 50 nm). The point defects created in the hills do not contribute to development of the defect structure, because they are annihilated almost completely by recombination of vacancies and interstitials or by movement to the surface sink. Under the hollows, vacancies which escaped recombination remain and the interstitial atoms, which are highly mobile even at low temperatures, migrate far from there to aggregate under the hills. The hills develop to walls by the interstitial atoms migrating from the surround. The remaining vacancies may move to the hollowed surface during implantation, which deepen the hollows. Honeycomb-like structure is formed in such a manner.

Now let us discuss the experimental results by the above-mentioned mechanism. The thickness of the heavily strained region formed in the upper part of the matrix (50 nm) is nearly equal to the range of point defect production, according to calculation with the TRIM code[13] where 6.2 eV and 7.5 eV[16] were adopted as the threshold energies for displacement of Ga and Sb. From this, it is concluded that the bottom surface of the cell was the effective surface for implantation, and that

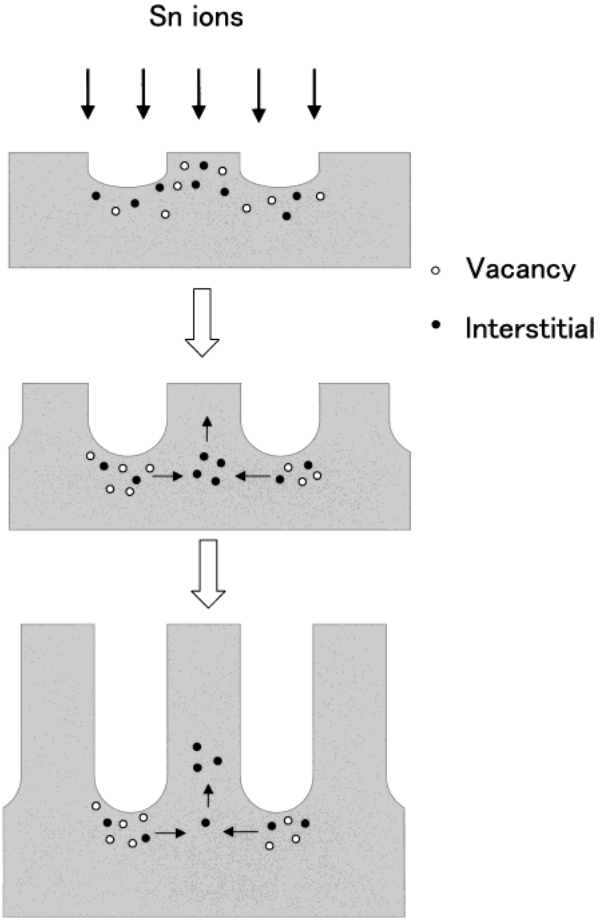

Fig. 7 The defect formation mechanism is shown. The point defects created on the hills do not contribute to the development of the defect structure. Under the hollows, the vacancies remaining after recombination are left there and the surviving interstitial atoms migrate and aggregate under the hills to increase their height.

sputtering and evaporation of the surface atoms or surface diffusion scarcely occur. Therefore the atoms for growth of the wall are considered to be supplied through the bottom of it from the matrix.

We now estimate the quantity of point defects required for formation of the defect structure. In Sample 1, the volume of the walls formed is $1 \times 10^{-5}\,\mathrm{cm}^3$ per surface area of $1\,\mathrm{cm}^2$, which corresponds to about 3×10^{17} constituent atoms. The TRIM simulation estimates that the number of implantation-induced interstitials is $2 \times 10^{18}\,\mathrm{cm}^{-2}$. In our proposed model, it is required that about 15% of the interstitials contribute to the formation of the walls (this value may be smaller considering the contribution of the remaining vacancies). This is probable, because the recombination of interstitials and vacancies is not effective as shown by the active formation and development of voids in ion-implanted GaSb.[11] The distribution of Ga and Sb concentrations in the wall (Fig. 5) is explained by the difference in mobility between Ga and Sb interstitials. If the mobility of Ga interstitials is larger than that of Sb, the Ga concentration will be high at the top of the surface and low at the lower part of the wall as shown in Fig. 5.

The difference in crystal structure between the upper and lower parts of walls does not contradict the proposed mechanism. Although the walls first grow in crystalline structure, they are amorphized during growth under the continuous irradiation of ions. As a result, the upper part becomes amorphous completely and the crystalline structure partly remains in the lower part as shown by Fourier transformation in Fig. 4.

The growth of the wall is generally considered as difficult because of the increase in surface energy. However, a similar phenomenon are the metal whiskers that grow in solid phase from their base. According to Frank's idea,[17] the growth of whiskers needs a supply of atoms by diffusion and stress for climbing dislocations (in order to supply atoms in the growth direction)-these two factors are satisfied in the case of GaSb–Sn^+. The interstitials are continually supplied to the base of the walls from the surround by ion implantation, and the heavy stress is induced in the implanted region as observed by TEM.

Amorphization has often been considered to be indispensable for swelling, as experiments have shown that there is a critical dose for swelling in GaSb ion implanted at room temperature,[10] and craters are formed in the Ge surface after amorphization.[15] However amorphization is not necessarily required in our proposed formation mechanism. In the above systems, the structure will have become amorphous at the ion dose when the point defects and the stress were stored long enough to drive the wall growth.

Void formation is one of the possible causes for formation of hollows and hills in the early stage of implantation. It has been suggested that the voids were formed near the surface, and they crossed the surface, resulting in the formation of cavities.[14] However, if the difference in the mobility between interstitials and vacancies is large enough, hollows and hills are formed in the early stage of implantation (at the dose of 10^{15}–$10^{16}\,\mathrm{ions/m}^2$ = one ion per $50\,\mathrm{nm} \times 50\,\mathrm{nm}$). Results strongly supporting the void mechanism are not yet obtained in our TEM and SEM study. In our present experiments, we did not examine the structure in the early stage of implantation. We will clarify the mechanism by subsequent work on samples with low ion doses that is now in progress.

5. Conclusion

The structure and the composition of the surface defect formed on (100)GaSb by 60 keV Sn^+ ion implantation at 150–153 K was studied by FE-TEM, FE-SEM, EDX and Fourier transformation of HRTEM images. Many cells with about 50 nm diameter were formed like a honeycomb on the surface implanted with a dose of $8.9 \times 10^{18}\,\mathrm{ions/m}^2$ and partitioned by walls with about 10 nm thickness. The depth of the cells was 220–250 nm, which is ten times larger than the implanted ion range. The upper part of the partitioning wall is amorphous and rich in Ga, while the lower part shows crystalline spots coinciding with the matrix. Under the surface defect, there is a heavily strained layer with about 50 nm thickness. The formation of this defect structure is a phenomenon similar to the anomalous behaviors observed in irradiated GaSb. We proposed a defect formation mechanism assuming a large difference in mobility between the interstitials and the vacancies induced by ion implantation, supported by experimental results and previous work.

Acknowledgements

We appreciate the contributions to the experimental works by Ms. A. Takano and Ms. K. Chikamori who were students at Kochi University of Technology. We would like to thank Mr. N. Baba and Ms. S. Komatsu of KOCHI CASIO CO., LTD for their kind help with scanning electron microscope observation. We also thank Dr. K. Shiramine for his kindness on several important references.

REFERENCES

1) D. J. Mazey and R. S. Nelson: Radiation Effects **1** (1969) 229–239.
2) D. K. Sadana: Nucl. Instrum. Methods Phys. Res. **B7/8** (1985) 375–386.
3) M. Taniwaki, H. Koide, N. Yoshimoto, T. Yoshiie, S. Ohnuki, M. Maeda and K. Sassa: J. Appl. Phys. **67** (1990) 4036–4041.
4) M. Taniwaki, H. Koide, T. Yoshiie, Y. Hayashi and H. Yoshida: J. Non-Cryst. Solids **117/118** (1990) 745–748.
5) M. Taniwaki, M. Yanaba, T. Yoshiie and Y. Hayashi: Defect Diffus. Forum **95/98** (1993) 989–994.
6) M. Taniwaki, T. Yoshiie, H. Koide, M. Ichihasi, N. Yoshimoto, H. Yoshida and Y. Hayashi: J. Appl. Phys. **66** (1989) 161–164.
7) D. Kleitman and H. J. Yearian: Phys. Rev. **108** (1957) 901.
8) Y. Homma: J. Vac. Sci. Technol. **A5** (1987) 321–326.
9) S. J. Pearton, A. R. Von Neida, J. M. Brown, K. T. Short, L. J. Oster and U. K. Chakrabarti: J. Appl. Phys. **64** (1988) 629–636.
10) R. Callec, P. N. Favennce, M. Salvi, H. L'Haridon and M. Gauneau: Appl. Phys. Lett. **59** (1991) 1872–1874.
11) R. Callec and A. Poudoulec: J. Appl. Phys. **73** (1993) 4831–4835.
12) M. Taniwaki, Y. Hayashi and T. Yoshiie: Proc. Int. Corf. On Solid-Solid Phase Transformations '99 (1999) 425–428.
13) J. P. Biersack and L. G. Haggmark: Nucl. Instrum. Methods **174** (1980) 257–269.
14) I. H. Wilson: J. Appl. Phys. **53** (1982) 1698–1705.
15) B. R. Appleton, O. W. Holland, D. B. Poker, J. Narayan and D. Fathy: Nucl. Instrum. Methods Phys. Res. **B7/8** (1985) 639–644.
16) K. Thommen: Phys. Rev. **174** (1968) 938–945; erattum, Phys. Rev. **179** (1969) 920.
17) F. C. Frank: Phil. Mag. **44** (1953) 854–860.